Multislice CT Virtual Intravascular Endoscopy for Assessing Pulmonary Embolisms: a Pictorial Review

Zhonghua Sun, PhD[1]
Sultan Ayed Al Dosari, MSc[1]
Curtise Ng, PhD[1]
Ali al- Mumntshari, PhD[2]
Saud Almaliky, RT[3]

[1]Discipline of Medical Imaging, Department of Imaging and Applied Physics, Curtin University of Technology, Perth, Western Australia, Australia;
[2]Department of Radiology, Kind Saud Hospital, Riyadh, Saudi Arabia;
[3]Department of Radiology, Military hospital, Riyadh, Saudi Arabia

Address reprint requests to:
Zhonghua Sun, PhD, Discipline of Medical Imaging, Department of Imaging and Applied Physics, Curtin University of Technology, GPO Box, U1987, Perth, Western Australia 6845, Australia.
Tel. +61-8-9266 7509
Fax. +61-8-9266 2377
e-mail: z.sun@curtin.edu.au

Multislice CT has been widely used in clinical practice for diagnosing cardiovascular disease due to its reduced invasiveness and its high spatial and temporal resolution. As a reliable alternative to conventional pulmonary angiography, multislice CT angiography has been recognized as the first line technique for detecting and diagnosing pulmonary embolism. A pulmonary embolism located in the main pulmonary artery, as well as being located in the segmental branches, can be accurately detected with multislice CT imaging, and especially with the use of 16- and 64-slice CT scanners. Visualization of pulmonary embolisms has traditionally been limited to 2D, multiplanar reformation and the 3D external surface visualizations. In this pictorial review, we present our experience of using 3D virtual intravascular endoscopy (VIE) to characterize and evaluate the intraluminal appearance of pulmonary embolisms in a group of patients who were suspected of having pulmonary embolism and who were undergoing multislice CT angiography. We expect that the research findings from this study will provide insight into the extent of disease and the luminal changes to the pulmonary arteries that are due to the presence of thrombus, and so monitoring of the progress of disease and predicting the treatment outcome can well be achieved.

C onventional pulmonary angiography has traditionally been regarded as the gold standard for making the diagnosis of pulmonary embolism (PE). However, it is not only an invasive procedure with a risk of mortality (0.5%) and morbidity (6%) (1, 2), but it also lacks diagnostic accuracy as subsegmental clots are not always recognized and interobserver disagreement occurs in up to one third of the cases (3). Contrast-enhanced pulmonary MR angiography has been shown in a number of studies to allow the diagnosis of PE with an accuracy equivalent to that of CT pulmonary angiography (4, 5). However, MR angiography is not widely used due to lack of availability, the long acquisition times and the difficulty of monitoring patients in the MR scanning room, despite its advantages over CT for the reasons of a lack of ionizing radiation and the lack of potentially nephrotoxic contrast medium (6). With the rapid developments of CT techniques, CT pulmonary angiography (CTPA) was initially used as an adjunct and then as an alternative to other imaging modalities (7), and it has recently been widely recognized as the method of choice for diagnosing suspected PE due to its superior sensitivity and specificity as compared to ventilation-perfusion isotope scanning (8–10). Moreover, CTPA allows a quantitative assessment that correlates well with the clinical severity, and CTPA has good interobserver agreement.

The early studies that used single slice and 4-slice CTPA have reported limited diagnostic accuracy or limited visualization of subsegmental clots (11, 12). However, CTPA with defined multislice CT (MSCT) protocols and using 16-and 64-slice CT

allows better identification of both central and peripheral thrombi (9, 11, 13). For visualizing a pulmonary embolism with CTPA, the 2D axial and multiplanar reformatted images are the most commonly used visualization tools in standard clinical practice. The main disadvantage of these views is the lack of direct intraluminal demonstration of the thrombus or the artery wall changes. Thus, the purpose of this study was to explore the potential applications of CTPA-generated virtual intravascular endoscopy (VIE) for visualizing pulmonary embolisms with regard to their intraluminal appearance or the luminal changes. VIE has previously been reported to be valuable for assessing aortic aneurysm and endovascular stent grafts as it offers additional information when compared to the conventional 2D views (14–16). We extended the applications of VIE to a group of patients who were suspected of having PE and their expected outcome would lead to better patient follow-up and management.

The Patients' Data and the Multislice CTPA Protocol

Twenty three (12 women and 11 men, mean age: 47 years, range: 14–83) consecutive patients suspected of having PE and who were referred for multislice CT angiography were included in this study. Ten patients underwent 16-slice CT pulmonary angiography (LightSpeed16, GE Healthcare, Milwaukee, WI, USA) with the scanning protocol as follows: 120 kVp, 200–250 mAs, a beam collimation of 16×0.625 mm, a gantry rotation time of 500 ms, reconstruction of the slice thickness 1.0–1.25 mm,

a pitch of 0.2–0.3 with a reconstruction interval of 0.5 or 0.6 mm. Thirteen patients underwent 64-slice CT pulmonary angiography (Brilliance 64, Philips Medical Systems, Best, the Netherlands) with the scanning protocol as follows: 120 kVp, 200–250 mAs, a beam collimation of 64×0.625 mm, a gantry rotation time of 420 ms, reconstruction of the slice thickness 0.6–1.25 mm, a pitch of 0.2–0.3 with a reconstruction interval of 0.4 or 0.6 mm. A field of view of 300–350 mm, a matrix size of 512×512 and $180°$ linear interpolation algorithms were used to reconstruct the images, resulting in an in-plane resolution of 0.58 mm $\times$ 0.58 mm–0.68 mm $\times$ 0.68 mm. All of the CTPA scans were performed with intravenously injecting 60 to 100 ml of non-ionic contrast medium (Omnipaque 350, Schering, Berlin, Germany) and this was administered at a flow rate of 5 ml/s. The scan was initiated using a bolus tracking technique with a threshold of 100 HU over baseline at the main pulmonary trunk.

Generation of the Virtual Intravascular Endoscopy (VIE) Images

All the datasets were burned onto CDs from the MSCT scanner and these were transferred to a separate workstation for generating the VIE images. The MSCT volume data was converted from the original DICOM (Digital Imaging and Communication in Medicine) images with using the commercially available software Analyze V 7.0 (Analyze V, AnalyzeDirect, Inc., Lexana, KS, USA). The details of generating the VIE images of the artery lumen
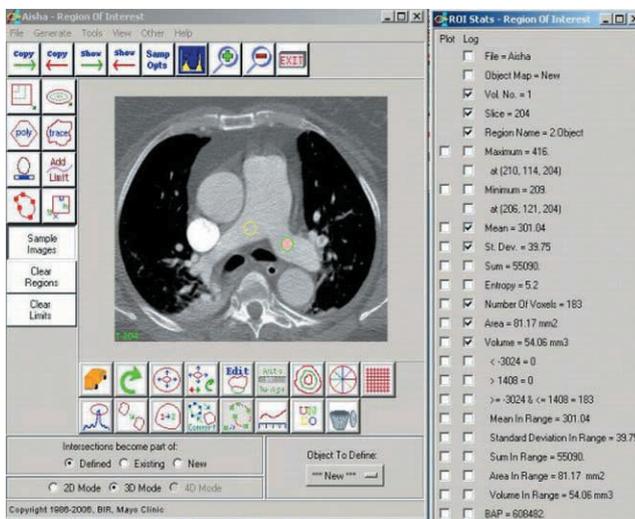

Fig. 1. Measurement of the signal to noise ratio (SNR). A circular region of interest with a minimum area of 50 mm² is placed at the bilateral main pulmonary arteries to measure the mean CT attenuation and image noise, and the latter is described as standard deviation (SD). The SNR is calculated by dividing the CT attenuation by the SD.
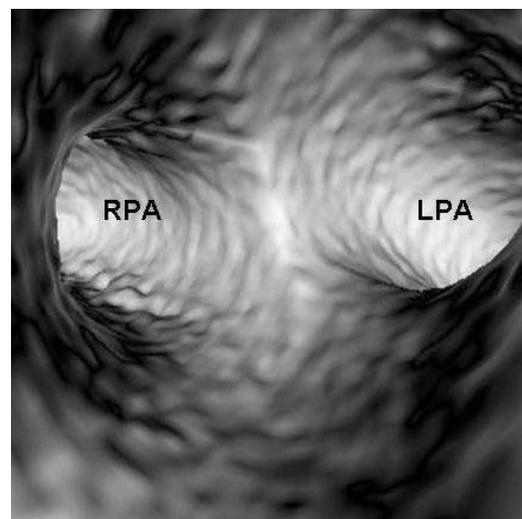

Fig. 2. Normal main pulmonary arteries visualized on VIE. LPA-left pulmonary artery, RPA-right pulmonary artery. The measured SNRs were 19 and 24 at the right and left pulmonary arteries, respectively.

A   **B**
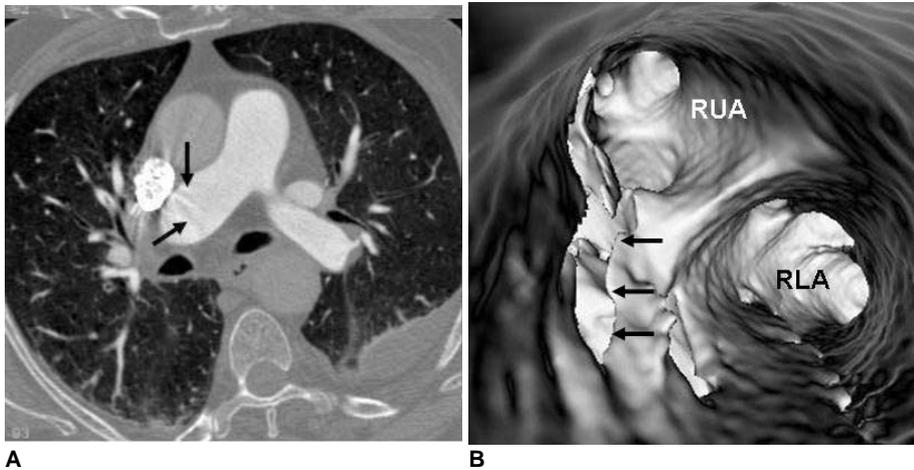
Fig. 3. VIE visualization of the PE in the right pulmonary artery is affected by the high density contrast in the superior vena cava. The measured SNR was 8.9 at the right pulmonary artery. Beam-hardening streak artifact (arrows in **A**) causes an irregular appearance of the right pulmonary artery visualized on VIE (**B**). The corresponding orthogonal views confirm that the irregular luminal change (**C**) is caused by the artefact. The arrows in 3B and C indicate the irregular wall changes that are due to artifact. RUA-right upper lobar artery, RLA-right lower lobar artery.

C
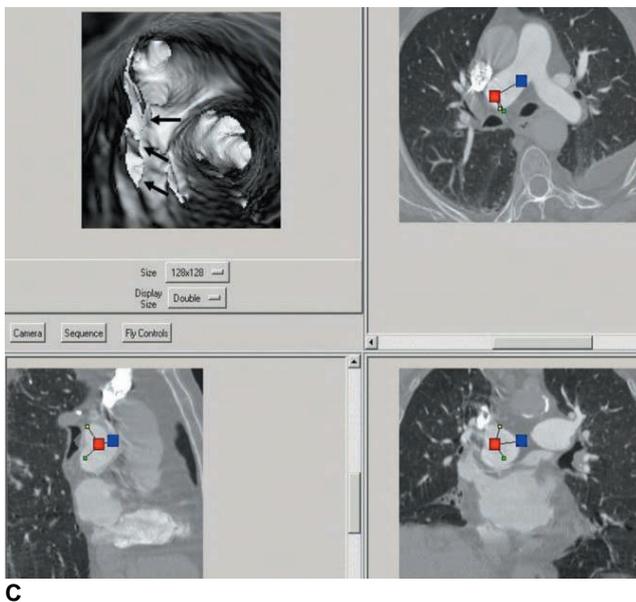
have been described elsewhere (14, 15). Similar to the previous studies, we used a CT number thresholding technique to produce endoscopic views of the pulmonary artery and its branches, as well as endoscopic views of the abnormal changes (14, 15). This was determined by select-ing the appropriate threshold value through measuring the CT attenuation at the left and right main pulmonary arteries. An upper threshold of 200–250 HU was applied to remove the contrast-enhanced blood from the vessel while keeping the thrombus and vessel lumen.

Measurements of the Image Noise and Image Quality

To assess the image quality of the multislice CTPA images, the image noise and the CT attenuation of the main pulmonary artery, as well as the signal to noise ratio (SNR), were determined in each patient. Image noise was

A   **B**
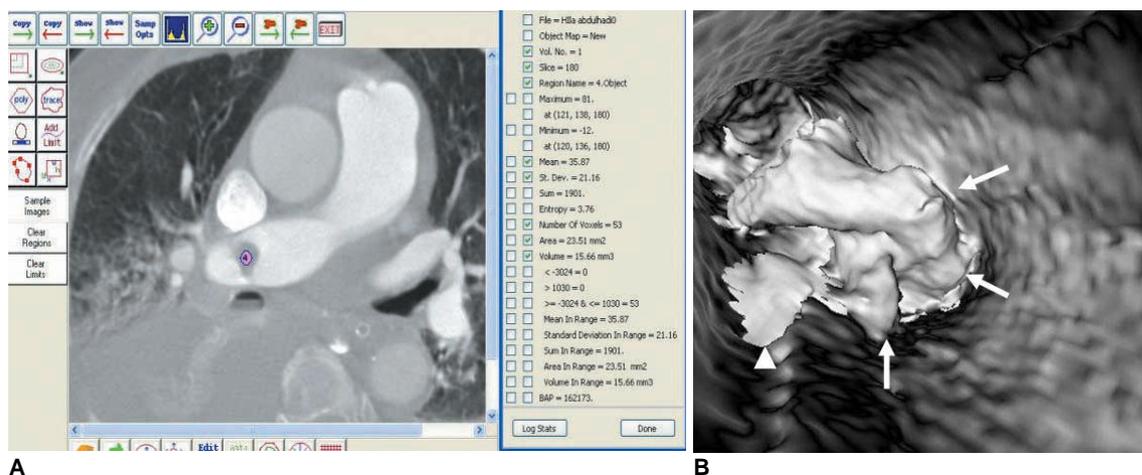
Fig. 4. VIE visualization of a pulmonary embolism in the right main pulmonary artery. The CT attenuation of the thrombus is measured to be 35.87 HU (**A**), and it appears as a protruding sign (arrows in **B**) inside the pulmonary artery after applying the upper CT threshold of 250 HU to remove the contrast-enhanced blood. The arrowhead refers to the artifacts caused by the high density in the superior vena cava.

defined as the standard deviation (SD) of the CT density in a region of interest (ROI) that was placed in the pulmonary artery (Fig. 1). The ROI was chosen to be placed in the centre of the pulmonary artery with a minimum area of 50 mm2 while carefully avoiding inclusion of the artery wall or thrombus to prevent any partial volume effects. The SNR was determined by dividing the mean attenuation by the image noise.

The mean SNR measured at the left and right pulmonary arteries was 14.2 + 4.6 and 14.4 + 5.4, respectively, for the 16-slice CTPA protocol, and it was 24.7 + 10.7 and 20 + 7.4, respectively, for the 64-slice CTPA protocol. The SNR was significantly different between the 16-and 64-slice CTPA protocols when it was measured at the left pulmonary artery ($p = 0.014$), but there was no significant difference when the SNR was measured at the right pulmonary artery ($p = 0.134$).

VIE Visualization of a Normal Pulmonary Artery

VIE was successfully generated in all of the patients. The VIE image quality was determined by the SNR measured at the pulmonary artery and its branches. The VIE image of the pulmonary artery with a high SNR shows a smooth intraluminal appearance (Fig. 2), while the VIE image of the pulmonary artery with a low SNR shows a smooth irregular appearance of the pulmonary artery wall (Fig. 3).

VIE Visualization of Pulmonary Embolisms

In this study, pulmonary embolism is recognized as a thrombus within the pulmonary vessel and it has CT attenuation much lower (less than 50 HU) than that of the contrast enhanced blood in the pulmonary artery (300–400 HU). Thus, when applying a CT threshold (the upper
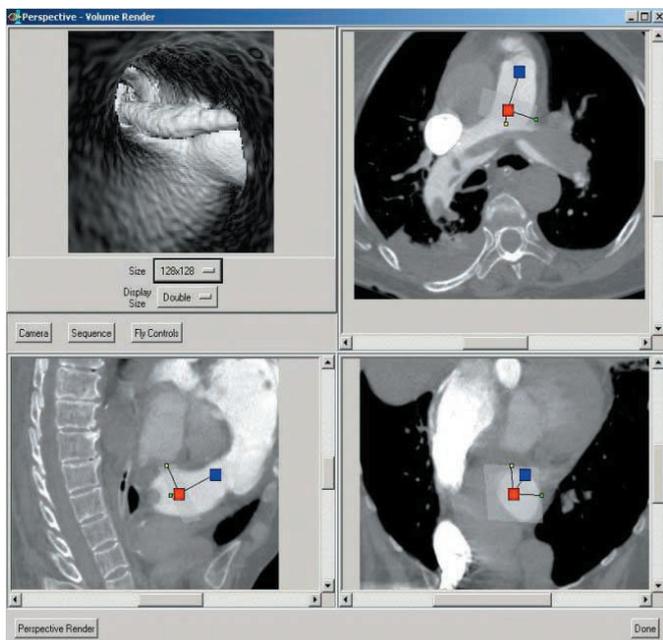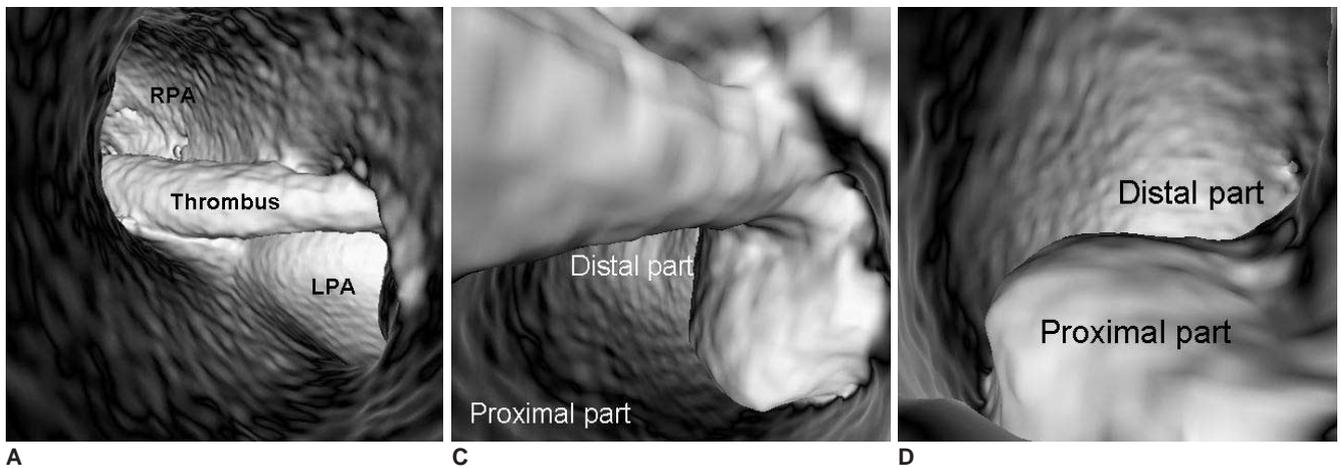
Fig. 5. A pulmonary embolism involving the bilateral pulmonary artery branches. A large thrombus is present in the left main pulmonary artery and it extends to the right side (**A**). The orthogonal views show that the viewing position is located in the pulmonary trunk (**B**). Figs 5 **C** and **D** demonstrate the continuous extension of the thrombus from the proximal part of the main pulmonary artery to the distal segment with lumen narrowing, as well as the protruding sign in the lumen.

threshold was normally chosen to be 200–300 HU) to remove the contrast-enhanced blood from the pulmonary artery, the low attenuation thrombus was kept together with the pulmonary wall and lumen in the generated VIE views. Thus, pulmonary embolism appears as an intraluminal protrusion arising from the wall (Fig. 4).

Pulmonary Embolism-the Main Pulmonary Artery Level

The presence of pulmonary embolism in the main pulmonary arteries is easily identified and visualized on the vessels that underwent VIE. The thrombus can be located in either one of the main pulmonary arteries (Fig. 4), and it is imaged as the appearance of a central protrusion within the pulmonary artery or it extends from one side of the pulmonary artery to the other side, depending on the extent of the pulmonary embolism (Fig. 5). The extent of the embolism can be assessed on VIE images by following the path of the thrombus from the proximal pulmonary artery to the distal or segmental branches.

Pulmonary Embolism-Lobar Artery Level

A thrombus located at the lobar artery level is also easily recognized on the VIE images as the protrusion sign arising from the arterial wall that corresponds to the affected lobar artery branches (Figs. 6, 7). When multiple pulmonary emboli are present in the lobar arteries, correlation with the orthogonal views (including the axial, coronal and sagittal reformatted images) is necessary to determine which lobar artery branch is involved (Fig. 6).

### Pulmonary Embolism-the Segmental and Subsegmental Levels

Due to its unique feature of providing intraluminal views and generating a virtual fly-through of the blood vessel, even if in the presence of severe stenosis, VIE is able to identify the pulmonary embolism in the segmental or subsegmental branches (Figs. 8, 9). In order to accurately confirm the location of a pulmonary embolism at the segmental or subsegmental levels, the observers need to correlate the VIE visualization with the corresponding orthogonal views to determine which pulmonary branches are involved as it is sometimes difficult to accurately identify the pulmonary artery ostia inside the pulmonary lumen, and especially when it comes to the subsegmental levels. The VIE images not only reveal the presence of thrombus within the arterial lumen, but they also clearly demonstrate the involvement of the segmental artery branches (Figs. 8, 9).

Single Embolism Versus Multiple Emboli

A single embolism was found in 18 cases with involvement of either the main pulmonary artery or the lobar or segmental branches, while multiple emboli were noticed in
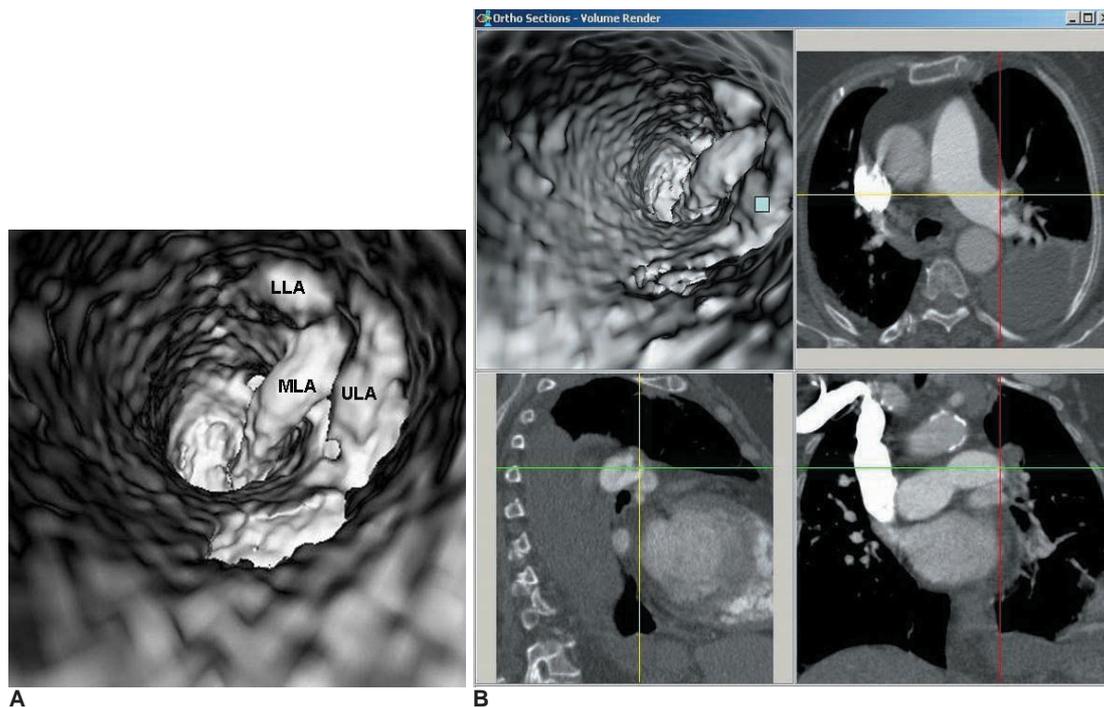
Fig. 6. VIE visualization of multiple emboli in the left lobar arteries (**A**). The multiplanar views help to confirm that the location of the thrombus corresponds to the involved lobar artery (**B**). ULA-upper lobar artery, MLA-middle (lingular) lobar artery, LLA-lower lobar artery. The blue box indicates the viewing position placed at the left upper lobar thrombus.
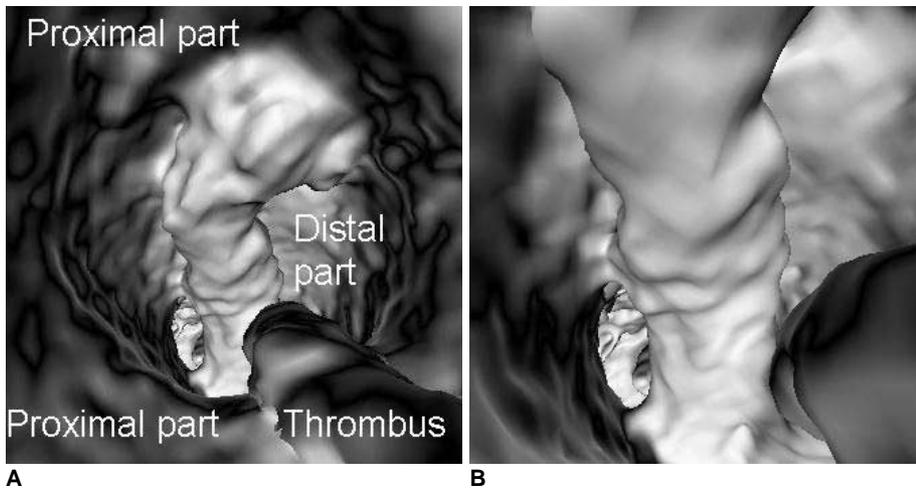
Fig. 7. The VIE views of the left lower lobar embolism from the proximal to distal segments of the lobar artery (**A, B**). The accurate position of the thrombus is confirmed with using the multiplanar views (**C**).

C
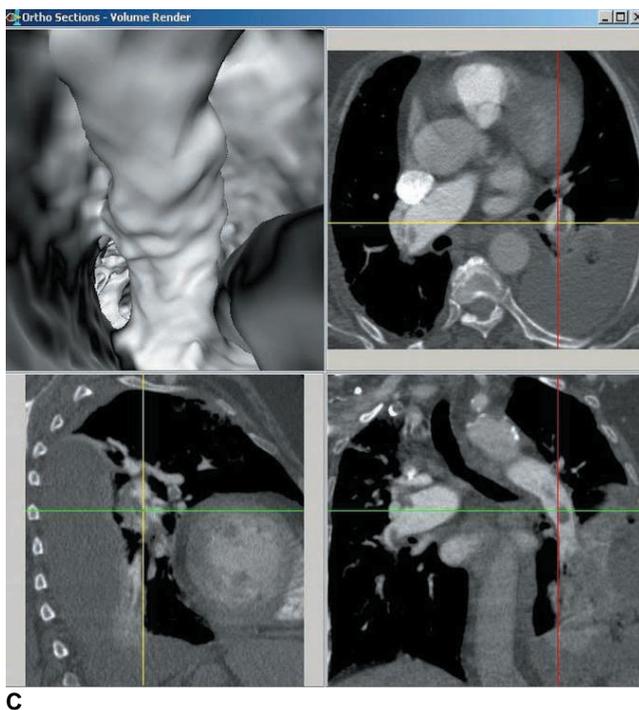
with the diagnosis of PE is motion artefact, but any motion artefact was not noticed in our patients.

DISCUSSION

Although our study is based on a small number of cases, our findings provide insight into the intraluminal appearances of pulmonary embolism with the aid of VIE visualization. In contrast to the conventional 2D or 3D extraluminal views, VIE allows for uniquely demonstrating the thrombus, whether it is located in the main pulmonary artery or in the lobar or segmental branches. This is especially useful for identifying a thrombus in the segmental or subsegmental arteries as an embolism located at these side branches is sometimes difficult to detect on CT images. Combined with the 2D views, VIE is able to confirm the thrombus in the distal pulmonary branches. Moreover, VIE visualization allows for a virtual fly-through of the entire pulmonary tree, which is valuable for assessing the extent of disease. However, the VIE images must be combined with the corresponding orthogonal views to confirm the segmental or subsegmental pulmonary embolism as it is difficult to determine the exact location of these branches based on the VIE image alone.

VIE has been reported to be useful to follow-up the endovascular stent graft repair of aortic aneurysm (14–18). VIE has additional value to demonstrate the intraluminal appearance of aortic stent grafts or fenestrated vessel stents in relation to the aortic branches, and mainly the renal arteries. VIE can enhance endovascular specialists' understanding of the treatment outcome of an endovascular repair of aortic aneurysm. To the best of our knowledge, there have been no studies performed regarding the application or diagnostic value of VIE for assessing pulmonary embolism. Our preliminary experience shows

5 cases, and these emboli involved the bilateral pulmonary artery branches. Multiple emboli were present in the main pulmonary artery, and they extended to the lobar and segmental branches in 3 cases (Figs. 5 and 6), while in the remaining 2 cases, only the lobar or segmental pulmonary arteries were involved.

Factors Affecting the VIE Image Quality

VIE visualization of the pulmonary artery and thrombus is mainly affected by the high contrast enhancement in the superior vena cava. The streaking artefacts arsing from the superior vena cava interfered with VIE visualization of the right pulmonary artery in nearly half of the cases, leading to the irregular wall appearance in the right main pulmonary artery. Another common factor that interferes

that VIE is not only able to demonstrate the intraluminal appearance of a pulmonary embolism, but it also assesses the extent of disease. The main potentials of providing direct demonstration of the intraluminal thrombus or the arterial wall changes by VIE lie in the following aspects, which we believe are useful from the clinical perspective:

- Accurately determining the location and extent of the pulmonary embolism, and especially for the cases with segmental or subsegmental embolism, where conventional 2D or 3D visualizations have limitations.
- Diagnosing and confirming a pulmonary embolism in indeterminate cases.
- Quantitatively evaluating the pre-and post-treatment of a thrombus and so this contributes to assessing the treatment outcome and predicting the progress of

disease.
- Dynamically assessing a pulmonary embolism via a virtual fly-through instead of using the static views, and this is considered to be valuable for assessing the severely occluded or near totally occluded branches.

The VIE image quality is determined by the degree of contrast enhancement in the pulmonary artery, yet the visualization of the right pulmonary artery is affected, to some extent, by the high-density contrast medium in the superior vena cava. Artifacts, and especially those at the right pulmonary artery, may interfere with the VIE visualization of the intraluminal appearance of a pulmonary embolism. Thus, artifacts could cause difficulty to differentiate the thrombus from the artifacts. However, a pulmonary embolism normally presents as a protruding

A   **C**   **D**

B
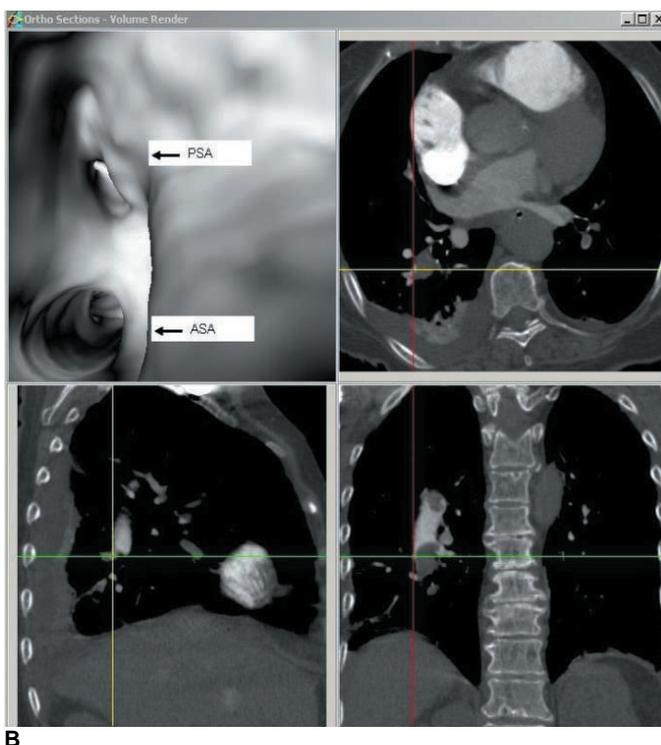
Fig. 8. The VIE views of the right posterobasal segmental embolism. The thrombus extends from the right lower lobar artery (**A**) to the posterobasal segmental arteries (**B, C**). The corresponding orthogonal view confirms that the position of the thrombus is located in the right posterobasal segmental artery with compressing the corresponding posterobasal segmental artery (**D**). ASA-anteromedial basal segmental artery, PSA-posterobasal segmental artery.
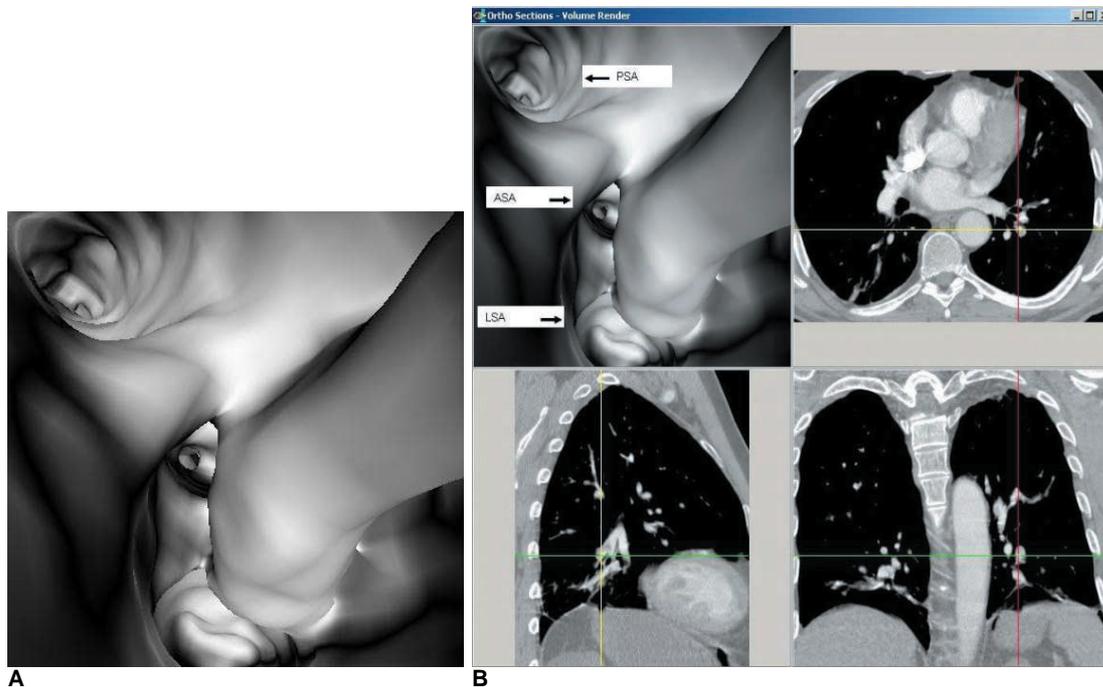
Fig. 9. The VIE views of the left lower pulmonary segmental embolism involving two arterial branches. The left lateral basal and antero-medial basal segmental arteries become narrowed due to the presence of the thrombus (**A**), while the left posterobasal segmental artery is normal. The corresponding orthogonal views (**B**) confirm the relationship between the thrombus and the segmental artery branches. ASA-anteromedial basal segmental artery, LSA-lateral basal segmental artery, PSA-posterobasal segmental artery.

sign from the intact artery lumen without any disruption of the ???. In contrast, the artifacts result in an irregular appearance in the artery lumen or they may even lead to discontinuity of the lumen. Streaking artifact can be distinguished from a pulmonary embolism by recognizing its non-anatomic, poorly defined, radiating nature (Fig. 3A). The use of a "saline chase" in CTPA could be an effective strategy to dilute the contrast density in the superior vena cava while still acquiring the diagnostic images, but it minimizes the degree of artifacts.

Researchers have previously reported that respiratory motion artifacts can cause the misdiagnosis of pulmonary embolism, and respiratory motion artifacts are the most common cause of an indeterminate CTPA (19). Jones and Wittram (20) found motion artifacts to be responsible for 74% of the indeterminate CTPAs. Since the main cause of motion during CTPA is the inability of dyspneic patients to hold their breath during the scanning time, the development and increased use of 16- and 64-slice CT with their substantially faster scanning times should lower the number of indeterminate CTPA cases. Yavas et al. (21) in their recent study reported that the thoracic CT images were nondiagnostic for two of 112 patients due to lung motion. No motion artifacts were present in our patients, and this was mainly due to the fast scanning technique available with using 16-and 64-slice CT in this study.

In conclusion, we believe that VIE could be used as a complementary tool together with the conventional 2D visualizations for evaluating pulmonary embolisms, in terms of the quantitative assessment of thrombus changes after medical treatment, the intraluminal changes of the arterial wall that are due to thrombus and the extent of a pulmonary embolism.

References

1. Stein PD, Athanasoulis C, Alavi A, Greenspan RH, Hales CA, Saltzman HA, et al. Complications and validity of pulmonary angiography in acute pulmonary embolism. *Circulation* 1992;85:462-468
2. Mills SR, Jackson DC, Older RA, Heaston DK, Moore AV. The incidence, etiologies, and avoidance of complications of pulmonary angiography in a large series. *Radiology* 1980;136:295-299
3. Diffin DC, Leyendecker JR, Johnson SP, Zucker RJ, Grebe PJ. Effect of anatomic distribution of pulmonary emboli on interob-server agreement in the interpretation of pulmonary angiography. *AJR Am J Roentgenol* 1998;171:1085-1090
4. Meaney JF, Weg JG, Chenevert TL, Stafford-Johnson D, Hamilton BH, Prince MR. Diagnosis of pulmonary embolism with magnetic resonance angiography. *N Engl J Med* 1997;336:1422-1427
5. Oudkerk M, van Beek EJ, Wielopolski P, van Ooijen PM, Brouwers-Kyuper EM, Bongaerts AH, et al. Comparison of contrast-enhanced magnetic resonance angiography and conventional pulmonary angiography for the diagnosis of pulmonary embolism: a prospective study. *Lancet* 2002;359:1643-1647
6. Keilholz SD, Bozlar U, Fujiwara N, Mata JF, Berr SS, Corot C,

et al. MR diagnosis of a pulmonary embolism: comparison of P792 and Gd-DOTA for first pass perfusion MRI and contrast-enhanced 3D MRA in a rabbit model. *Korean J Radiol* 2009;10:447-454

7. British thoracic society guidelines for the management of suspected acute pulmonary embolism: british thoracic society standards of care committee pulmonary embolism guideline development group. *Thorax* 2003;58:470-484

8. Hayashino Y, Goto M, Noguchi Y, Fukui T. Ventilation-perfusion scanning and helical CT in suspected pulmonary embolism: meta-analysis of diagnostic performance. *Radiology* 2005;234:740-748

9. Guilabert JP, Manzur DN, Tarrasa MJ, Llorens ML, Braun P, Arques MP. Can multislice CT alone run out reliably pulmonary embolism? A prospective study. *Eur J Radiol* 2007;62:220-226

10. Schoepf UJ, Goldhaber SZ, Costello P. Spiral computed tomography for acute pulmonary embolism. *Circulation* 2004;109:2160-2167

11. Rathbun SW, Raskob GE, Whitsett TL. Sensitivity and specificity of helical computed tomography in the diagnosis of pulmonary embolism: a systematic review. *Ann Intern Med* 2000;132:227-232

12. van Strijen MJL, de Monye W, Kieft GJ, Pattynama PMT, Prins MH, Huisman MV. Accuracy of single-detector spiral CT in the diagnosis of pulmonary embolism: a prospective multicentre cohort study of consecutive patients with abnormal perfusion scintigraphy. *J Thromb Haemost* 2005;3:17-25

13. Perrier A, Roy PM, Sanchez O, Le Gal G, Meyer G, Gourdier AL, et al. Multidetector-row computed tomography in suspected pulmonary embolism. *N Engl J Med* 2005;352:1760-1768

14. Sun Z, Winder J, Kelly B, Ellis P, Hirst D. CT virtual intravascular endoscopy of abdominal aortic aneurysms treated with suprarenal endovascular stent grafting. *Abdom Imaging* 2003;28:580-587

15. Sun Z, Winder J, Kelly B, Ellis P, Kennedy P, Hirst D. Diagnostic value of CT virtual intravascular endoscopy in aortic stent grafting. *J Endovasc Ther* 2004;11:13-25

16. Sun Z, Ellen Y, Nadkarni S, Wright R, Hartley DE, Lawrence-Brown MMD. CT virtual intravascular endoscopy in the follow-up of fenestrated endovascular grafts. *J Endovasc Ther* 2008;15:42-51

17. Sun Z. 3D multislice CT angiography in post-aortic stent grafting: a pictorial essay. *Korean J Radiol* 2006;7:205-211

18. Sun Z, Mwipatayi B, Allen Y, Hartley D, Lawrence-Brown M M. Multislice CT angiography of fenestrated endovascular stent grafting for treating abdominal aortic aneurysms: a pictorial review of the 2D/3D visualizations. *Korean J Radiol* 2009;10:285-293

19. Wittram C, Maher MM, Yoo AJ, Kalra MK, Shepard JA, McLoud TC. CT Angiography of pulmonary embolism: diagnostic criteria and causes of misdiagnosis. *Radiographics* 2004;24:1219-1238

20. Jones SE, Wittram C. The indeterminate CT pulmonary angiogram: imaging characteristics and patient clinical outcome. *Radiology* 2005;237:329-337

21. Yavas US, Calisir C, Ozkan IR. The interobserver agreement between residents and experienced radiologists for detecting pulmonary embolism and DVT with using CT pulmonary angiography and indirect CT venography. *Korean J Radiol* 2008;9:498-502